International Journal of Fluid Power 8 (2007) No. 1 pp. 39-49

ON THE APPLICATION OF OLEO-PNEUMATIC ACCUMULATORS FOR THE PROTECTION OF HYDRAULIC TRANSMISSION LINES AGAINST WATER HAMMER - A THEORETICAL STUDY

M. Galal Rabie

Modern Academy for Engineering and Technology, Cairo, Egypt
rrabie@idsc.net.eg

Abstract

The remarkable advance in hydraulic and electro hydraulic power systems resulted in producing high response control valves of very short settling time. The actuation of these valves rapidly opens or closes the hydraulic transmission lines, which may produce a severe pressure surge. This paper is dedicated to evaluate the applicability of oleo-pneumatic accumulators for the protection against this phenomenon. A lumped parameter model was developed for the transmission line, assuming different number of lumps, considering the effect of line resistance, inertia and capacitance. The validity of lumped parameter models is evaluated by comparing theoretical results with published experimental results. The paper presents the derivation of a closed expression for the size of the hydraulic accumulator needed to protect the transmission line against the destructive effect of the pressure surge. The study showed that the implementation of an accumulator of convenient size reduced the duration and amplitude of the transient pressure oscillations.

Keywords: hydraulic, accumulator, transmission line, water hammer, resistance, inertia, capacitance, compressibility, surge, capacitance, lumped parameter

1 Introduction

Surge or water hammer, as it is commonly known, is the result of a sudden change in liquid velocity; magnitude or direction. The resulting pressure surge can lead to catastrophic system component failure. The primary cause of water hammer in the fluid power systems is the quick closing valves. The hammer occurs because an entire train of liquid is being stopped so fast that the end of the train hits up against the front end and sends shock waves through the pipe. The pressure spike; acoustic wave, created by rapid valve closure can be of high values compared with the system pressure.

The study of hydraulic transients began with the investigation of sound wave propagation in air, followed by theories derived by Joukowski in 1900 and Allievi in 1903. Joukowski conducted extensive experiments on pipes with diameters ranging from 50mm to 150mm and lengths from 350m to 7620m. He developed a formula for the surge wave velocity, the rise of pressure and velocity reduction. He also discussed the effect of various closing rates of a valve. This phenomenon still receives serious and continuous attention due to its destructive effect. Among the most recent studies are the publications of Chaiko (2002) and Ravina (2006).

This paper is dedicated to the study of the pressure surge in hydraulic transmission lines and the way of protection using oleo-pneumatic accumulators.

2 Modelling of Hydraulic Transmission Lines

The hydraulic transmission line is actually a distributed parameter system. The motion of the liquid in the transient conditions takes place under the action of the fluid inertia, friction and compressibility as well as the acting pressure forces. The oil velocity, pressure and temperature vary from point to point along the pipe length and pipe radius. The mathematical model of line becomes too complicated when taking into consideration all of the variations of the oil and flow parameters. Therefore it is necessary to develop a simplified

This manuscript was received on 25 July 2006 and was accepted after revision for publication on 21 February 2007

mathematical model, which describes the dynamic behavior of the transmission line with acceptable accuracy. A fairly precise model is the lumped parameter model, presented in the publications of Karnopp (1972), Rabie (1986 and 1997), and Kassem (1988). The lumped parameter model was deduced considering the following assumptions:

The flow is laminar unidirectional.

The liquid pressure and velocity are looked at as the mean values, and are considered constant across the pipe section.

The oil moves in the line as one lump (single lump model) or several lumps (multi-lump model).

The fluid motion is affected by:

- the pressure forces,
- the line resistance due to friction forces,
- the inertia of the moving fluid,
- and the hydraulic capacitance (considering the fluid compressibility and the pipe walls elasticity).

The effect of the line resistance, inertia and capacitance are assumed to be localized in one of three separate portions in the line as shown by Fig. 1. The effect of the resistance of the whole line is localized in the first portion, the effect of the inertia of the whole line is localized in the second portion while the effect of the line capacitance takes place in the third portion.

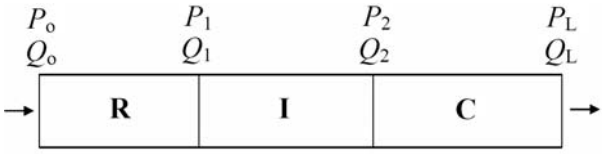

Fig. 1: *Single lump model of transmission line*

2.1 Hydraulic Resistance

In hydraulic transmission lines, the flow may be laminar or turbulent depending on the ratio of the inertia to the viscous friction forces. For laminar flow, Fig. 2, the pressure losses in the line are calculated as follows.

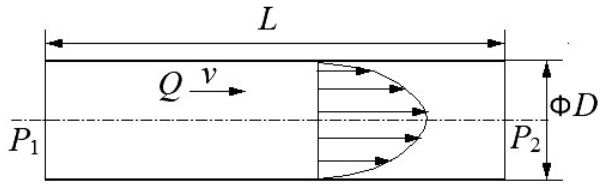

Fig. 2: *Laminar flow in pipeline*

$$\Delta P = \lambda \frac{L}{D} \frac{\rho v^2}{2} \tag{1}$$

where

$v = 4Q / \pi D^2$; Mean fluid velocity, m/s

$\lambda = 64 / Re$; Friction coefficient, for laminar flow

$Re = \rho v D / \mu$; Reynolds number

The following expression for the pressure losses was obtained by substituting for λ, v and Re.

$$\Delta P = P_1 - P_2 = \frac{128 \mu L}{\pi D^4} Q = R\,Q \tag{2}$$

The term R expresses the resistance of the hydraulic transmission line.

In the first portion of the transmission line, Fig. 1, the oil moves as one oil lump subjected to the friction forces. Therefore its motion is described by the following equations relating the pressures and flow rates at both ends of the first portion.

$$P_o - P_1 = RQ_o \tag{3}$$

$$Q_o = Q_1 \tag{4}$$

Applying Laplace's transform to these equations, then, after rearrangement, the following equation is obtained.

$$\begin{bmatrix} P_o(s) \\ Q_o(s) \end{bmatrix} = \begin{bmatrix} 1 & R \\ 0 & 1 \end{bmatrix} \begin{bmatrix} P_1(s) \\ Q_1(s) \end{bmatrix} = \mathbf{R} \begin{bmatrix} P_1(s) \\ Q_1(s) \end{bmatrix} \tag{5}$$

2.2 Hydraulic Inertia

Figure 3 shows a single oil lump, subjected to pressure difference $\Delta P = P_1 - P_2$. The effect of fluid inertia can be formulated, assuming incompressible non-viscous flow.

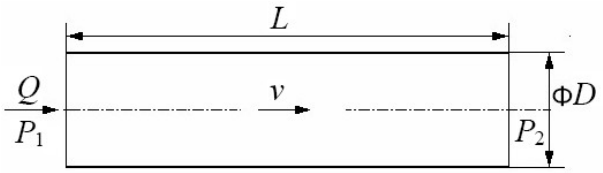

Fig. 3: *Single oil lump, subjected to pressure difference $\Delta P = P_1 - P_2$*

An expression for the line inertia is deduced as follows.

$$F = m\,a \tag{6}$$

$$\Delta P\, A = \rho\, A\, L \frac{dv}{dt} \tag{7}$$

$$\Delta P = \frac{\rho L}{A} \frac{dQ}{dt} = \frac{4 \rho L}{\pi D^2} \frac{dQ}{dt} = I \frac{dQ}{dt} \tag{8}$$

The term I expresses the inertia of the hydraulic transmission line.

The following relations describe the motion of the oil lump in the second portion of the hydraulic transmission line, Fig. 1, under the action of its inertia, I.

$$P_1 - P_2 = I \frac{dQ_1}{dt} \tag{9}$$

$$Q_1 = Q_2 \tag{10}$$

Applying Laplace's transform to Eq. 9 and 10, then, after rearrangement, the following equation is obtained.

$$\begin{bmatrix} P_1(s) \\ Q_1(s) \end{bmatrix} = \begin{bmatrix} 1 & Is \\ 0 & 1 \end{bmatrix} \begin{bmatrix} P_2(s) \\ Q_2(s) \end{bmatrix} = \mathbf{I} \begin{bmatrix} P_2(s) \\ Q_2(s) \end{bmatrix} \tag{11}$$

2.3 Hydraulic Capacitance

The liquid compressibility is defined as the ability of liquid to change its volume when its pressure varies. For pure liquid, the relation between the oil volume and pressure variations is described by the following formula.

$$B = -\frac{\Delta P}{\Delta V / V} \text{ or } \Delta V = -\frac{V}{B}\Delta P \tag{12}$$

The bulk modulus B of pure oil is nearly constant. It is slightly affected by the system pressure. However, when the oil includes bubbles of gases, air or vapors, the bulk modulus of this mixture decreases due to the high compressibility of gases. If the total volume of mixture is V_T, the gas volume is αV_T and the oil volume is $(1-\alpha)V_T$, the following expression for the equivalent bulk modulus B_e of the mixture could be systematically deduced.

$$\frac{1}{B_e} = \frac{\alpha}{nP} + \frac{1-\alpha}{B} \tag{13}$$

The effect of compressibility can be formulated by considering a single oil lump in hydraulic transmission line, Fig. 4. The oil is assumed to be subjected only to the effect of oil compressibility. The pressure in the line is P, inlet flow rate is Q_1 and outlet flow rate is Q_2. The variation of pressure P leads to the changes in oil volume due to the oil compressibility and the changes in pipe volume due to pipeline walls elasticity.

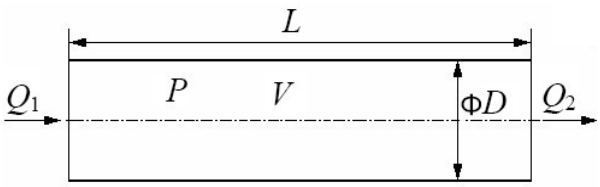

Fig. 4: *Single oil lump, subjected to oil compressibility*

The variation of oil volume in line due to inlet and outlet flow rates is ΔV_Q.

$$\Delta V_Q = \int (Q_1 - Q_2)dt \tag{14}$$

The variation of volume of oil in line due to the compressibility effect is ΔV_C.

$$\Delta V_C = -\frac{V}{B}\Delta P \tag{15}$$

The variation of volume of pipe line, ΔV_L depends on the line material, wall thickness and diameter, and the system pressure. The walls deform due to the combined effect of the radial and axial pressure forces. An expression for this volumetric variation due to a pressure increment ΔP is derived as follows.

Figure 5 illustrates the effect of pressure forces in the radial direction. The volume variation due to radial wall deformation, ΔV_{LR}, can be calculated as follows:

$$\sigma = \frac{\Delta PDL}{2hL} = \frac{\Delta PD}{2h} = E\varepsilon_r \tag{16}$$

$$\varepsilon_r = \frac{\pi\Delta D}{\pi D} = \frac{\Delta D}{D} \tag{17}$$

$$\Delta D = \frac{\Delta PD^2}{2Eh} \tag{18}$$

$$\Delta V_{LR} = \frac{\pi}{4}\left\{(D+\Delta D)^2 - D^2\right\}L = \frac{\pi L}{4}\Delta D(2D+\Delta D) \tag{19}$$

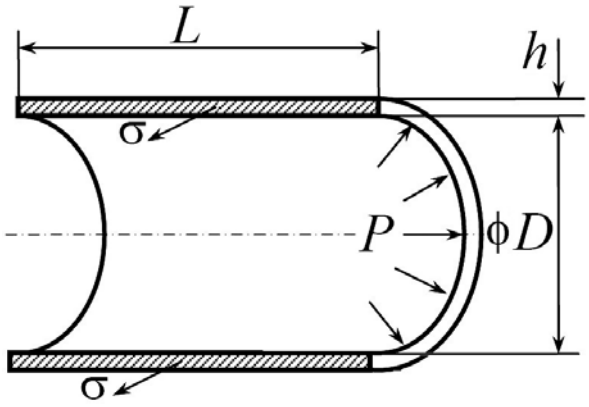

Fig. 5: *Radial deformation of the pipe wall*

Considering the actual parameters of the transmission lines used in hydraulic power systems, the term ΔD is negligible compared to $2D$. Therefore Eq.19 becomes:

$$\Delta V_{LR} = \frac{\pi}{4}D^2L\left(\frac{D}{Eh}\right)\Delta P \tag{20}$$

Figure 6 illustrates the effect of pressure forces in the axial direction. The following expression for the volumetric variation due to axial wall deformation, V_{LA}, can be systematically deduced.

$$\Delta V_{LA} = \frac{\pi}{4}D^2L\left(\frac{D}{4Eh}\right)\Delta P \tag{21}$$

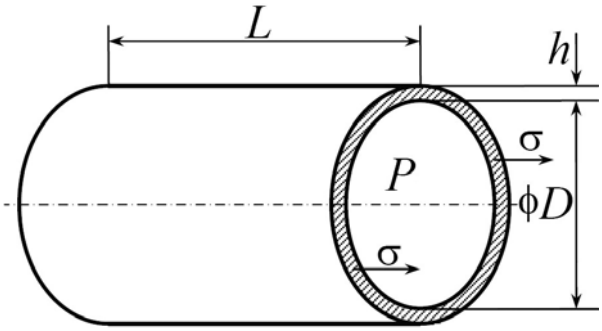

Fig. 6: *Axial deformation of the pipe wall*

The total variation of line volume is ΔV_L, where:

$$\Delta V_L = \Delta V_{LR} + \Delta V_{LA} = V\Delta P\left(\frac{5D}{4Eh}\right) \tag{22}$$

The total variation of oil volume ($\Delta V_Q + \Delta V_C$) is equal to the pipe volume variation ΔV_L .

$$\Delta V_Q + \Delta V_C = \Delta V_L \tag{23}$$

$$\int (Q_1 - Q_2)dt - \frac{V}{B}\Delta P = V\Delta P\left(\frac{5D}{4Eh}\right) \tag{24}$$

$$\int (Q_1 - Q_2)dt = V\left(\frac{1}{B} + \frac{5D}{4Eh}\right)\Delta P = C\Delta P \tag{25}$$

The term C expresses the capacitance of the hydraulic transmission line.

If the volumetric variation due to pipe deformation is negligible, then, the hydraulic capacitance becomes: $C = V/B$. Then, for the studied portion of the line, Fig. 4, the continuity equation has the following form:

$$Q_1 - Q_2 = \frac{d}{dt}(CP) = C\frac{dP}{dt} \tag{26}$$

Considering the effect of oil compressibility in the last portion, Fig. 1, the following relations could be deduced.

$$Q_2 - Q_L = C\frac{dP_L}{dt} \tag{27}$$

$$P_2 = P_L \tag{28}$$

Applying Laplace's transform to Eq. 27 and 28, then, after rearrangement, the following equation is obtained.

$$\begin{bmatrix} P_2(s) \\ Q_2(s) \end{bmatrix} = \begin{bmatrix} 1 & 0 \\ Cs & 1 \end{bmatrix}\begin{bmatrix} P_L(s) \\ Q_L(s) \end{bmatrix} = \mathbf{C}\begin{bmatrix} P_L(s) \\ Q_L(s) \end{bmatrix} \tag{29}$$

2.4 Transfer Functions of Transmission Lines

2.4.1 Single Lump Model

By eliminating the assumed internal variables, P_1, P_2, Q_1 and Q_2, Fig. 1, the following equation was obtained for a single lump model.

$$\begin{bmatrix} P_o \\ Q_o \end{bmatrix} = \mathbf{RIC}\begin{bmatrix} P_L \\ Q_L \end{bmatrix} = \begin{bmatrix} ICs^2 + RCs + 1 & Is + R \\ Cs & 1 \end{bmatrix}\begin{bmatrix} P_L \\ Q_L \end{bmatrix} \tag{30}$$

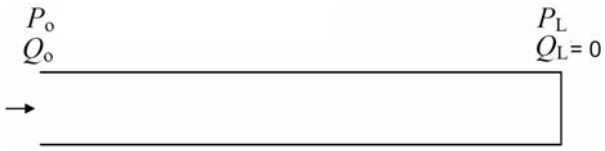

Fig. 7: *Closed end line*

In the case of a closed end line, Fig. 7, the transfer function relating the pressures at the two extremities is:

$$\frac{P_L}{P_o} = \frac{1}{ICs^2 + RCs + 1} \tag{31}$$

2.4.2 Two-Lump Model

Assuming more than one lump, the hydraulic resistance, inertia and capacitance of each lump, in an n-lump model are given by the following expressions.

$$\text{Lump resistance } R_n = \frac{128\mu(L/n)}{\pi D^4} \tag{32}$$

$$\text{Lump inertia } I_n = \frac{4\rho(L/n)}{\pi D^2} \tag{33}$$

$$\text{Lump capacitance } C_n = \frac{\pi D^2(L/n)}{4}\left(\frac{1}{B} + \frac{5D}{4Eh}\right) \tag{34}$$

Assuming two oil lumps, the fluid resistance, inertia and capacitance elements can be arranged as shown by Fig. 8.

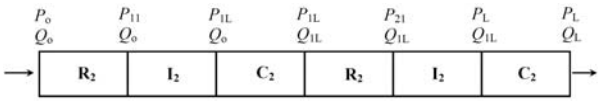

Fig. 8: *Two-Lump Model*

The following are the equations describing the two-lump model.

$$P_o - P_{11} = R_2 Q_o \tag{35}$$

$$P_{11} - P_{1L} = I_2\frac{dQ_o}{dt} \tag{36}$$

$$Q_o - Q_{1L} = C_2\frac{dP_{1L}}{dt} \tag{37}$$

$$P_{1L} - P_{21} = R_2 Q_{1L} \tag{38}$$

$$P_{21} - P_L = I_2\frac{dQ_{1L}}{dt} \tag{39}$$

$$Q_{1L} - Q_L = C_2\frac{dP_L}{dt} \tag{40}$$

The transfer matrix of the two-lump model can be deduced as follows.

$$\begin{bmatrix} P_o \\ Q_o \end{bmatrix} = [\,\mathbf{R_2 I_2 C_2}\,]^2\begin{bmatrix} P_L \\ Q_L \end{bmatrix} \tag{41}$$

$$\begin{aligned}\begin{bmatrix} P_o \\ Q_o \end{bmatrix} &= \begin{bmatrix} I_2C_2s^2 + R_2C_2s + 1 & I_2s + R_2 \\ C_2s & 1 \end{bmatrix}^2\begin{bmatrix} P_L \\ Q_L \end{bmatrix} \\ &= \begin{bmatrix} a_{11} & a_{12} \\ a_{21} & a_{22} \end{bmatrix}\begin{bmatrix} P_L \\ Q_L \end{bmatrix}\end{aligned} \tag{42}$$

Where:

$$a_{11} = I^2C^2s^4 + 2IRC^2s^3 + (R^2C^2 + 3IC)s^2 + 3RCs + 1 \tag{43}$$

$$a_{12} = I^2Cs^3 + 3IRCs^2 + (R^2C + 2I)s + 2R \tag{44}$$

$$a_{21} = IC^2s^3 + RC^2s^2 + 2Cs \tag{45}$$

$$a_{22} = ICs^2 + RCs + 1 \tag{46}$$

2.4.3 Three-Lump Model

The above treatment of the two-lump model can be applied systematically to deal with models of greater number of lumps. For three-lump model the transfer matrix is as follows.

$$\begin{bmatrix} P_o(s) \\ Q_o(s) \end{bmatrix} = [\,\mathbf{R_3\, I_3 C_3}\,]^3\begin{bmatrix} P_L \\ Q_L \end{bmatrix} \tag{47}$$

$$= \begin{bmatrix} I_3C_3s^2 + R_3C_3s + 1 & I_3s + R_3 \\ C_3s & 1 \end{bmatrix}^3 \begin{bmatrix} P_L(s) \\ Q_L(s) \end{bmatrix} = \begin{bmatrix} b_{11} & b_{12} \\ b_{21} & b_{22} \end{bmatrix} \begin{bmatrix} P_L(s) \\ Q_L(s) \end{bmatrix} \quad (48)$$

Where:

$$b_{11} = I^3C^3s^6 + 3I^2RC^3s^5 + (3IR^2C^3 + 5I^2C^2)s^4 + (10IRC^2 + R^3C^3)s^3 + (6IC + 5R^2C^2)s^2 + 6RCs + 1 \quad (49)$$

2.4.4 Four-Lump Model

The transfer matrix of the four-lump model is:

$$\begin{bmatrix} P_o(s) \\ Q_o(s) \end{bmatrix} = [\,\mathbf{R_4}\ \mathbf{I_4}\ \mathbf{C_4}\,]^4 \begin{bmatrix} P_L \\ Q_L \end{bmatrix}$$

$$= \begin{bmatrix} I_4C_4s^2 + R_4C_4s + 1 & I_4s + R_4 \\ C_4s & 1 \end{bmatrix}^4 \begin{bmatrix} P_L(s) \\ Q_L(s) \end{bmatrix} = \begin{bmatrix} c_{11} & c_{12} \\ c_{21} & c_{22} \end{bmatrix} \begin{bmatrix} P_L(s) \\ Q_L(s) \end{bmatrix} \quad (50)$$

Where

$$c_{11} = I^4C^4s^8 + 4I^3RC^4s^7 + (6I^2R^2C^4 + 7I^3C^3)s^6 + (21I^2RC^3 + 4IR^3C^4)s^5 + (15I^2C^2 + 21IR^2C^3 + R^4C^4)s^4 + (7R^3C^3 + 30IRC^2)s^3 + (15R^2C^2 + 10IC)s^2 + 10RCs + 1 \quad (51)$$

2.5 Validation of Lumped Parameter Models

The lumped parameter model was used to develop a computer simulation program for the transmission line. The simulation program was developed using the SIMULINK package and used to calculate the transient response of the hydraulic transmission line. The studied line has the following parameters; Length L = 18 m, inner diameter D = 10 mm, oil bulk modulus B = 1.95 GPa and oil density ρ = 868 kg/m^3, Fig. 9. The model validation process was conducted for four different cases. In each case, the transient response of the transmission line was calculated and compared with published results of measurements conducted on a line of the same parameters, Lallement (1976).

2.5.1 First Case

The studied line is connected to a constant pressure source by a 2/2 DCV (a), Fig. 9. The DCV (b) connects the line to the tank through a throttle valve. In the first case of study, the experiment started by closing the DCV (a) then the valve (b). The initial pressure value in the line is zero. The valve (a) is rapidly opened to connect the constant pressure source, of 447 bar, to the line inlet. The dynamic viscosity of oil μ = 0.1215 Ns/m^2 and the equivalent Bulk modulus of oil B_e = 1.96 GPa.

The studied line resistance, inertia and capacitances are: R = 8.912x10^9 Pa s/m^3, I =1.989 x10^8 kg/m^4 and C = 7.213x10^{-13}m^5/N

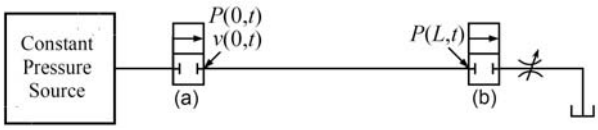

Fig. 9: *Scheme of the connection of line*

The transient variation of the line-end pressure P(L,t), was calculated. The calculations were carried out using different lumped parameter models; 1, 2, 3 and 4-Lump models. The simulation and experimental results are plotted in Fig. 10.

The precision of model was evaluated by examining of how close is its response to the experimental results. The difference between the theoretical and the experimental results was evaluated by calculating the percentage of the integral of absolute difference (IAD), defined as:

$$IAD = \frac{\int_0^T \left| P_{Lth} - P_{Lexp} \right| dt}{P_{Lss}T} \times 100\% \quad (52)$$

The study of Fig. 10 shows satisfactory agreement between the simulation and the experimental results for the 4-lump model.

2.5.2 Second Case

In the second case, the valves (a and b) were initially opened. The constant supply pressure was 80 bar and the throttle valve was adjusted to produce a mean inlet oil velocity of 5 m/s. The valve (b) was rapidly closed and the transient variation in inlet oil velocity was calculated. Figure 11 carries the simulation and experimental results. The study of this figure shows that the four-lump model gives acceptable agreement with the experimental results.

2.5.3 Third and Fourth Cases

In these two cases, the valves (a and b) were initially opened. The throttle valve was adjusted to produce a mean inlet oil velocity of 3 m/s.

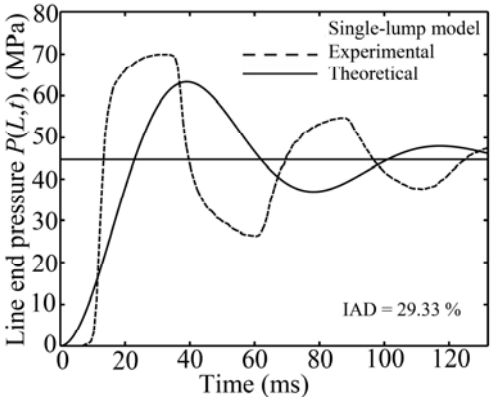

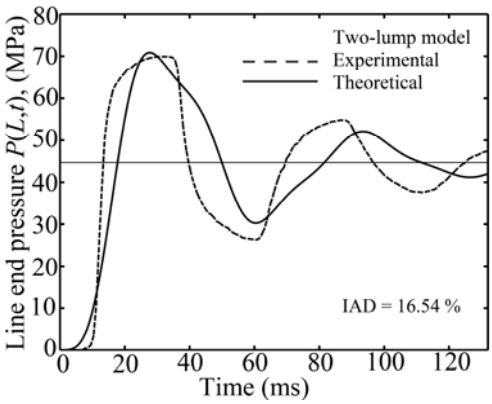

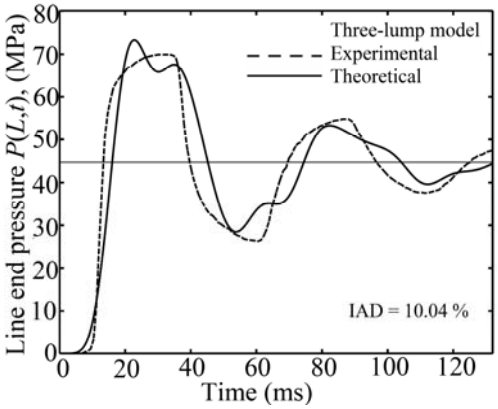

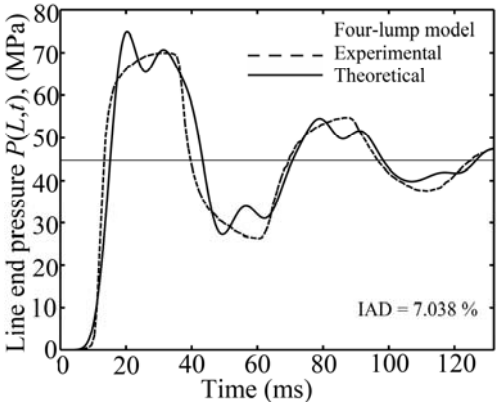

L = 18 m, D = 10 mm, B = 1.95 GPa, P_o= 447 bar, ν = 116 cSt, ρ = 868 kg/m^3

Fig. 10: *Step response of closed-end hydraulic transmission line described by 1,2,3 and 4-lump models, for step input pressure of 44.7 MPa*

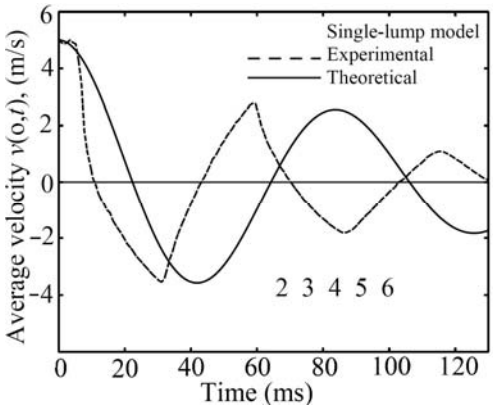

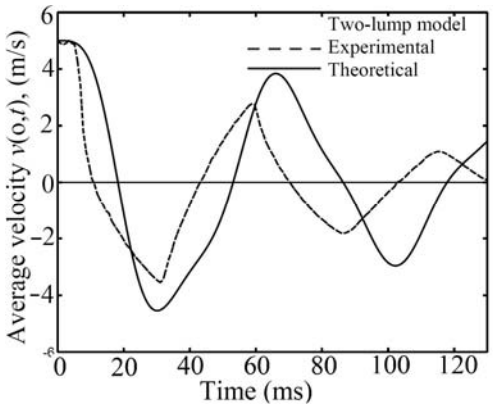

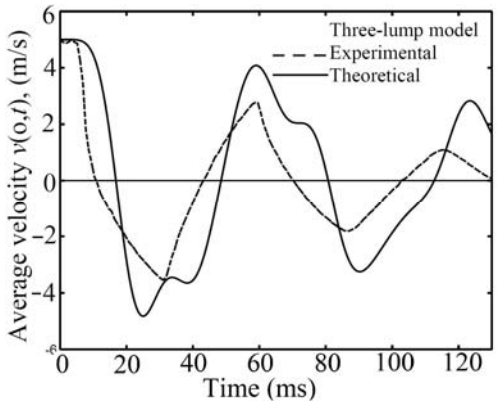

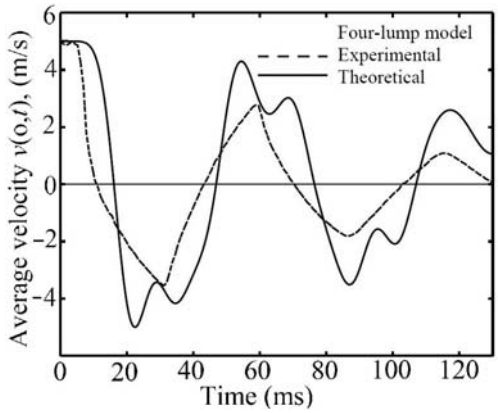

L = 18 m, D = 10 mm, B = 1.95 GPa, P_o= 80 bar, ν = 116 cSt, ρ = 868 kg/m^3

Fig. 11: *Step response of Line-inlet oil velocity to step closure of end throttle valve, v_i = 5 m/s*

The third case has a constant supply pressure of 44.7 MPa and oil kinematic viscosity $\nu = 116$ cSt while these values were 8 MPa and 56 cSt for the fourth case. The valve (b), Fig. 9, was rapidly closed and the transient variation of line end pressure P(L,t) was calculated. Figures 12 and 13 carry the simulation and experimental results of the third and fourth cases respectively.

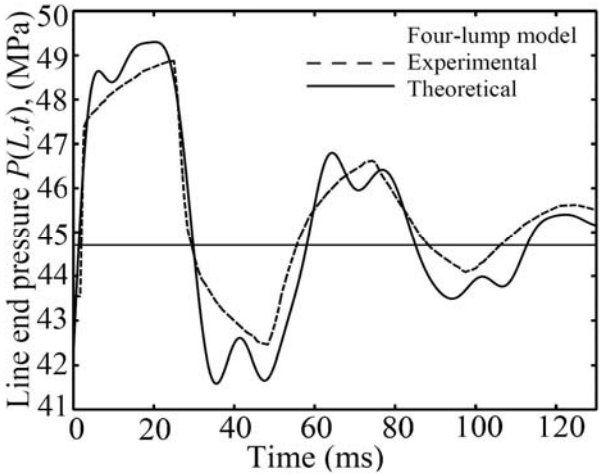

L = 18 m, D = 10 mm, B_e =1.96 GPa, p_o= 447 bar, ν = 116 cSt, ρ = 868 kg/m^3, c=1500 m/s

Fig. 12: *Step response of Line-End pressure to step closure of end throttle valve, v_i = 3 m/s*

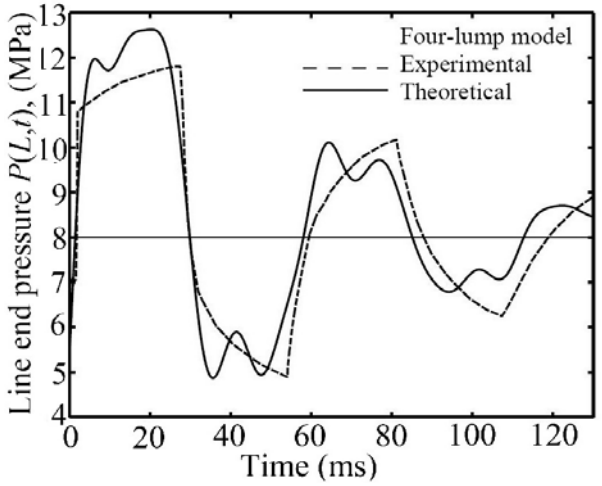

L = 18 m, D = 10 mm, B = 1.95 GPa, p_o= 80 bar, ν = 56 cSt, ρ = 868 kg/m^3, c =1500 m/s

Fig. 13: *Step response of Line-End pressure to step closure of end throttle valve, v_i = 3 m/s*

The study of Figs. 10 to 13 shows that the four-lump model describes, with acceptable accuracy, the dynamic behavior of hydraulic transmission lines. The transient response of this model agrees with the experimental response with acceptable precision, mainly, on the level of the maximum overshoot and the frequency and damping of the transient oscillations. Moreover, the validity of the four-lump model was evaluated on the bases of frequency response calculations, Rabie (1986 and 1997). These studies considered the flow in a pipe and between two coaxial pipes. The results showed that the four-lump model describes with good precision the first, dominant, mode of the line resonance from the point of view of the resonance frequency and damping.

Admittedly, the models developed on the basis of distributed parameters assumptions are more precise. There are efficient distributed models that can be used for simulation. But these models require software that can handle system with delay signals efficiently. Thus, the distributed parameter models cannot be applied without further complicating the overhaul system model. Moreover, the lumped parameter model is easily implemented in bond graph models. Therefore, this study is based on a four-lump model.

3 Absorption of Hydraulic Shocks

The rapid closure of control valves results in rapid deceleration of fluid columns. When the fluid lines are long enough, the resulting pressure shock may lead to dangerous effects.

Consider that the oil is moving with a mean speed v in a line of cross-sectional area A and length L. The end of line is closed rapidly during time period t_c. The valve closure creates a pressure wave, which propagates through the line. The time period t_p is that needed for the travel of the pressure wave to the line end and return back; $t_P = 2L/c$, where c is the sound speed in the fluid. If $t_c \le t_P$, then the pressure at the valve inlet increases and the line is subjected to a hydraulic shock.

If the valve is suddenly closed, a pressure wave travels up the pipe with velocity c. During a short time interval (dt) an element of liquid of length L is brought to rest. Therefore, an expression for the decelerating force acting on the oil and the pressure rise at the valve inlet could be deduced as follows.

$$F = m\frac{dv}{dt} \tag{53}$$

$$PA - (P + dP)A = \rho A c dt \frac{dv}{dt} \tag{54}$$

$$dP = -\rho c dv$$

or

$$\Delta P = -\rho c \Delta v \tag{55}$$

When the liquid is fully stopped, $\Delta v = -v$, then:

$$\Delta P = \rho v c\,. \tag{56}$$

If the closure time t_c is greater than the pressure wave propagation time t_P, ($t_c > t_P$), the peak pressure could be calculated approximately as follows.

$$\Delta P = \frac{t_P}{t_c}\rho v c = \frac{2L}{t_c}\rho v \tag{57}$$

These expressions show that the pressure rise due to the sudden closure of line is independent of the steady state pressure. This result agrees with the experimental results published by Lallement (1976). The maximum overshoot pressures are equal, regardless of the steady state pressure. The experimentally recorded overshoot is about 40 bar Fig. 12 and 13, while the value calculated using Eq. 57 is 39.06 bar.

Therefore, when it is not feasible to close the valve slowly, surge tanks or hydraulic accumulators are used to absorb all or most of the pressure rise. When using the hydraulic accumulator to absorb the resulting hydraulic shock, it should be fitted as close as possible to the source of the shock. The size of the accumulator should be calculated such that it can effectively absorb the hydraulic shock. Figure 14 shows a hydraulic accumulator installed near to the control valves to protect the transmission line against hydraulic shocks.

Initially, before the valve closure, the steady state pressure at the accumulator inlet (line end) is P_1. The valve closure increases the pressure to P. This pressure increase starts to decelerate the moving liquid. The application of Newton's second law to the moving mass of liquid yields:

$$(P - P_1)A = -\rho AL\frac{dv}{dt} \tag{58}$$

$$(P - P_1) = -\rho L\frac{dv}{dt} \tag{59}$$

The oil flows into the accumulator due to the pressure increase resulting from the rapid valve closure. Consider the most possible severe operating conditions, where the valve is closed within almost zero time period. The oil flows into the accumulator with an initial flow rate, Av, then:

$$\frac{dV_L}{dt} = Av \tag{60}$$

If the Accumulator size is V_o, the volume of oil in the accumulator is V_L and the gas volume is V, then:

$$V + V_L = V_o = Const. \tag{61}$$

$$\frac{dV}{dt} = -\frac{dV_L}{dt} = -Av \tag{62}$$

$$dV = -Av\,dt \tag{63}$$

Then; $$(P - P_1)dV = \rho ALvdv \tag{64}$$

The accumulator is installed to limit the maximum pressure to a maximum value of P_2. An expression for the size of the needed accumulator can be deduces as follows:

For isothermal process:

$$PV = P_oV_o = const. \tag{65}$$

$$dV = -\frac{P_oV_o}{P^2}dP \tag{66}$$

$$(P - P_1)(-\frac{P_oV_o}{P^2})dP = \rho ALvdv \tag{67}$$

Thus $$\int_{P_1}^{P_2}(\frac{1}{P} - \frac{P_1}{P^2})dP = -\frac{\rho AL}{P_oV_o}\int_v^0 vdv \tag{68}$$

$$V_o = \frac{\rho AL v^2}{2P_o\left\{\ln\left(\frac{P_2}{P_1}\right) + \frac{P_1}{P_2} - 1\right\}} \tag{69}$$

Where P_1 and P_2 are the initial and maximum pressures, respectively

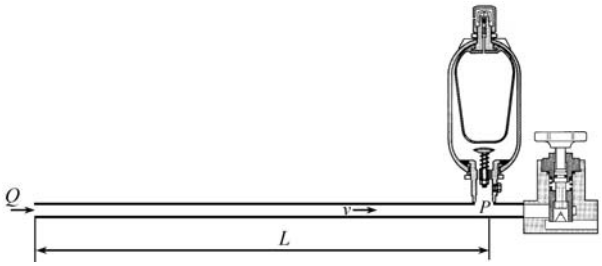

Fig. 14: *Functional scheme of accumulator used for protection against pressure shocks*

For polytropic process:

$$dV = -\frac{P_o^{1/n}V_o}{n\,P^{\frac{n+1}{n}}}dP \tag{70}$$

$$(P - P_1)\left(-\frac{P_o^{1/n}V_o}{n\,P^{\frac{n+1}{n}}}\right)dP = \rho ALvdv \tag{71}$$

$$\int_{P_1}^{P_2}(P^{-\frac{1}{n}} - P_1P^{-\frac{n+1}{n}})dP = -\frac{n\rho AL}{P_o^{1/n}V_o}\int_v^0 vdv \tag{72}$$

$$V_o = \frac{n\rho AL v^2/\left(2P_o^{1/n}\right)}{\frac{n}{n-1}\left(P_2^{(n-1)/n} - P_1^{(n-1)/n}\right) + n\left(P_1P_2^{-1/n} - P_1^{(n-1)/n}\right)} \tag{73}$$

These expressions for the accumulator size were derived neglecting the effect of the fluid compressibility and the pipe wall elasticity. The friction losses in the line and accumulator inlet local losses were also neglected. The friction and local pressure losses assist the fluid deceleration, while the walls elasticity and oil compressibility would accept some oil during the transient periods. Therefore, when neglecting these parameters, the deduced formulae results in an accumulator size greater than that actually required. Nevertheless, it is safer and counts for the possible approximations and calculation inaccuracy.

The application of oleo-pneumatic accumulators for the protection against hydraulic shocks was investigated here. The proper accumulator size was calculated using Eq. 73. The following are the parameters of the studied system, Fig. 15.

Diameter	= 1 cm
Length	= 18 m
Oil density	= 868 kg/m^3
Kinematic Viscosity	= 56 cSt
Bulk modulus	= 1.6 GPa
Inlet constant pressure	= 8 MPa
Initial line-end pressure	= 6.2 MPa
Accumulator charging pressure	= 5.1 MPa
Initial oil velocity	= 6 m/s
Polytropic exponent	= 1.3
Allowable end pressure increment	= 2.2 MPa
Accumulator size, calculated	= 126 cm^3
Line capacitance; C	= 8.84x10^{-13} m^3/Pa
Line inertia; I	= 1.99x10^8 kg/m^4
Line resistance; R	= 3.56x10^9 Ns/m^5

The equations describing the line are given in section 2.4. When the accumulator is installed, the equation describing the last capacitor (Eq. 40 for the two-lump model) should be replaced by the equations describing the accumulator as follows:

$$V = V_o - \int (Q_{IL} - Q_L) dt \tag{74}$$

$$P_L = P_o (V_o / V)^n \tag{75}$$

Fig. 15: *Scheme of the studied system*

The studied line was supplied by pressurized oil at constant pressure. The line-end directional DCV was open and the throttle valve was partially opened to control the oil speed at 6 m/s. The DCV is shut at $t = 0.2$s. Figure 16 shows the transient variation of line-end pressure in the two cases; with and without accumulator.

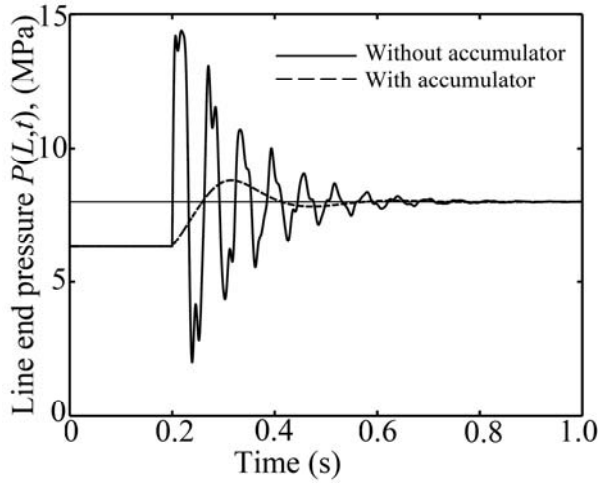

Fig. 16: *Transient response of the transmission line to sudden closure of the exit valve*

In the case of line without accumulator, the transient response shows an overshoot of 63.9 bar and settling time of 353 ms. The installation of hydraulic accumulator reduced the pressure overshoot to 8 bar and the settling time to 169 ms. In addition to this improvement, the transient response oscillations are substantially reduced, which provides an important increase in the fatigue life of the pipe.

The effect of accumulator size was investigated by calculating the Integral Error Squared (*IES*), defined as:

$$IES = \int_0^T (P_L - P_{Lss})^2 dt \tag{76}$$

The calculation results are shown in Fig. 17 which shows that the *IES* increases as the accumulator volume becomes less than or greater than a certain value (0.152 liters here).

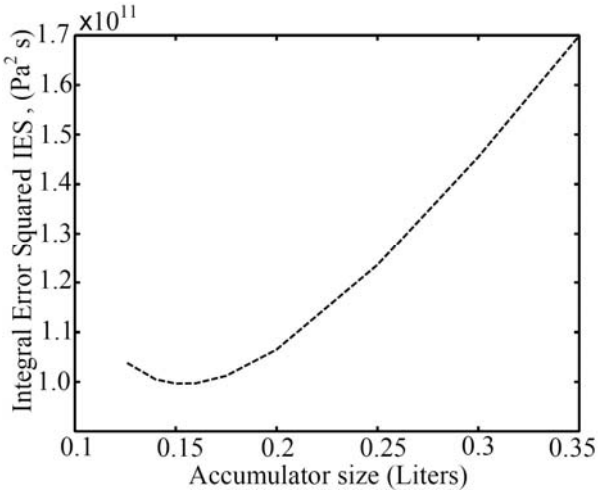

Fig. 17: *Effect of accumulator size on the Integral error squared of the transient response*

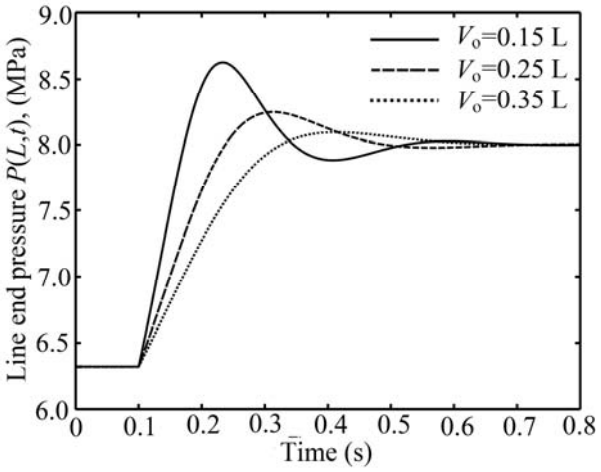

Fig. 18: *Step response of the transmission line equipped with a hydraulic accumulator of different sizes*

The effect of accumulator size on the IES can be explained as follows. The greater size of accumulator decreases the system stiffness and, consequently, decreases its natural frequency. Meanwhile, the system resistance is not affected by the accumulator size, which results in an increased damping coefficient. Thus, the increase in accumulator size results in more damped response and consequently increased IES. The reduction of accumulator size reduces the damping coefficient and leads to greater maximum percentage overshoot and increased *IES*, Fig. 18. Therefore, both of the minimum *IES* and maximum percentage overshoot should be considered when selecting the proper accumulator size. The minimum value of *IES* was obtained for the accumulator size estimated by Eq. 73.

4 Conclusion

This paper is dedicated to the evaluation of the effectiveness of oleo-pneumatic accumulators in the protection of the hydraulic lines against hydraulic shocks. The line was described by a four-lump model. The validity of lumped parameter model is evaluated

by comparing theoretical results with published experimental results. The paper presents a derivation of an expression for the recommended size of the hydraulic accumulator needed to protect the transmission line against the destructive effect of pressure surge. The study showed that the installation of the accumulator too close to the valve reduced the duration and amplitude of the transient pressure oscillations. The accumulator size, calculated by the deduced closed equation, produced an optimum line response, according to the integral error squared criterion.

Nomenclature and Abbreviations

A	Line cross-sectional area	[m^2]
A, a	Acceleration	[m/s^2]
B	Bulk modulus of oil	[Pa]
B_e	Equivalent bulk modulus of fluid	[Pa]
C	Whole line capacitance	[m^3/Pa]
$\boldsymbol{C}$	Capacitance matrix	
c	Sonic speed	[m/s]
D	Line inner diameter	[m]
DCV	Directional control valve	
F	Force	[N]
I	Whole line Inertia	[kg/m^4]
$\boldsymbol{I}$	Inertia matrix	
IAD	Percentage integrated absolute difference	[%]
L	Pipe length	[m]
m	Mass	[kg]
n	Polytropic exponent	
P	Pressure	[Pa]
P_1	Minimum, or initial, operating pressure	[Pa]
P_2	Maximum operating pressure	[Pa]
P_L	Line-end pressure	[Pa]
P_{Lexp}	Pressure at the closed end, experimental	[Pa]
P_{Lss}	Steady state pressure at the closed end	[Pa]
P_{Lth}	Pressure at the closed end, theoretical	[Pa]
P_o	Accumulator charging pressure	[Pa]
ΔP	Pressure losses or pressure difference	[Pa]
Q	Flow rate	[m^3/s]
R	Whole line resistance	[Ns/m^5]
$\boldsymbol{R}$	Resistance matrix	
Re	Reynolds number	
T	Considered time duration of response	[s]
t_c	Valve closure time	[s]
t_p	Pressure wave propagation time	[s]
v	Mean fluid velocity	[m/s]
V	Initial oil volume	[m^3]
V_L	Liquid volume in accumulator	[m^3]
V_o	Accumulator size	[m^3]
ΔV	Volume change due to pressure variation	[m^3]
μ	Dynamic viscosity	[Pa s]
ν	Kinematic viscosity	[m^2/s]
α	Ratio of gas content in mixture	
λ	Friction coefficient	
ρ	Oil density	[kg/m^3]

References

Chaiko, M. A. and **Brinckman, K. W.** 2002. Models for Analysis of Water Hammer in Piping with Entrapped Air, *ASME, Journal of Fluids Engineering*, March, Volume 124, Issue 1, pp. 194-204.

Karnopp, D. 1972. Bond Graph Models for Fluid Dynamic Systems, *ASME Journal of Dynamic Systems, Measurement and Control*, Sept, pp. 222-229.

Kassem, S. A. et al. 1988. Dynamic Analysis of Hydraulic Transmission Lines by a Lumped Model, *Bulletin of Fac. of Eng.*, Ain Shams Univ., Vol. 22, No. 2, Mech. Eng., pp. 1-18.

Lallement, J. 1976. Study of the Dynamic Behavior of Hydraulic Lines, (in French), *Les Memoir Techniques du Centre Technique des Industries Mecaniques CETIM*, France, No. 27, Sept.

Rabie, M. G. 1986. About the Lumped Parameter Approach to Hydraulic Line Modeling, Proceedings of *2nd AME Conf., M.T.C.*, Cairo, May 6-8, Vol. 1, paper (DYN 4), pp. 31-46.

Rabie, M. G. 1997. On the Validity of the Lumped Parameter Models for Fluid Flow between Coaxial Pipes, *AMSE Periodicals; Modeling, Measurement and Control*, B, AMSE Press, Lyon, France, Vol. 63, No. 1,2, pp. 31-47.

Ravina, E. 2006. Validation of High Performance Pneu-Hydraulic Shock Absorbers, the *IASTED Conference on Modelling, Identification, and Control* Lanzarote, Canary Islands, Spain Feb. 6-8.

Acknowledgement

The author is indebted to Mr Jaques Lallement, Jacques.Lallement@cetim.fr, Machine et command Dpt, Centre Technique des Industries Mecaniques CETIM, France, for his kind permission to use his experimental results in this paper.

Prof. Dr. M. Galal RABIE
Professor of Mechanical Engineering, Modern Academy for Engineering and Technology, Cairo, Egypt.

Previous occupations and Experience

- Professor of Mechanical engineering, Military Technical College (MTC), Cairo, Nov.1991.
- Head of Aircraft department, MTC.
- Head of Scientific Council of Aerospace Dpt,. MTC.
- Supervisor of 19 MSc and PhD Thesis.
- Author and coauthor of 5 text books.
- Author or coauthor of 45 papers